

# Bead, Hoop, and Spring as a Classical Spontaneous Symmetry Breaking Problem

Fredy Ochoa<sup>1\*</sup> and Jorge Clavijo<sup>2†</sup>

<sup>1</sup>Departamento de Física, Universidad Nacional de Colombia,

<sup>2</sup>Departamento de Ciencias Básicas, Escuela Colombiana de Ingeniería.  
Bogotá-Colombia

26th November 2024

## Abstract

We describe a simple mechanical system that involves Spontaneous Symmetry Breaking. The system consists of two beads constrained to slide along a hoop and attached each other through a spring. When the hoop rotates about a fixed axis, the spring-beads system will change its equilibrium position as a function of the angular velocity. The system shows two different regions of symmetry separated by a critical point analogous to a second order transition. The competitive balance between the rotational dynamics and the interaction of the spring causes an Spontaneous Symmetry Breaking just as the balance between temperature and the spin interaction causes a transition in a ferromagnetic system. In addition, the gravitational potential act as an external force that causes explicit symmetry breaking and a feature of first-order transition. Near the transition point, the system exhibits a universal critical behavior where the changes of the parameter of order is described by the critical exponent  $\beta = 1/2$  and the susceptibility by  $\gamma = 1$ . We also found a chaotic behavior near the critical point. Through a demonstrative device we perform some qualitative observations that describe important features of the system.

## I Introduction

Although gauge theories and Spontaneous Symmetry Breaking (SSB) [1] are rather abstract concepts which are associated with symmetries operating on internal degrees of freedom, their significance and nature emerges in a quite straightforward way through systems that exhibit geometrical properties associated with space-time symmetries, and that shares the same basic features as models with gauge structure. In the literature some works about analogies with classical systems are found [2], where different mechanical models are used to illustrate similar characteristics found in particle physics and solid state physics. In this work with a simple mathematical treatment, we describe another mechanical system that exhibits SSB and dynamical restitution of a discrete symmetry in a similar fashion as a second order phase transition. In contrast to the systems reported by the literature, our model is in a closer relation with a thermodynamic system in the sense that the former use the gravity as an essential external parameter to generate symmetry restitution, while ours may generate spontaneous breaking and restitution with only internal interactions, where the gravity act as an external field that causes explicit symmetry breaking, such as external interactions cause explicit breaking in thermal physics. The model shows not only interesting features that resembles to the SSB in gauge theories, but also in-

volves other related concepts. For example, it can be used in a basic level of classical mechanics as an application of rotational dynamics and to visualize the stability of systems from energy diagrams. In a higher level, it can be introduced as an example in the Lagrangian formulation of analytical mechanics. In a thermodynamic framework, this model illustrates the behavior of a first- and second-order transition according to the Tisza's definition. Furthermore, because of the nature of the SSB, this system exhibits a critical behavior near the transition point which belongs to the same universality class as a large number of thermodynamic systems. Thus, this problem may provide instructive insights that concern with more advanced topics into the classical study of the critical phenomena in phase transitions. In addition, the system presents interesting properties associated with nonlinear solutions, which may be source of chaotic behavior and generates a simple application into the theory of classical chaos.

## II Stability

We consider two identical beads of mass  $m$  that can slide without friction on a horizontal hoop of radius  $R$ . There appears a potential of interaction through a spring attached to both beads. The spring constant is  $k$  and its equilibrium length is less than the diameter of the hoop, i.e.  $2r_0 < 2R$ . The system is sketched in Fig. 1, where the position  $z_0$  of both beads is the same measured from the

---

\*e-mail: faochoap@unal.edu.co

†e-mail: eclavijo@escuelaing.edu.co

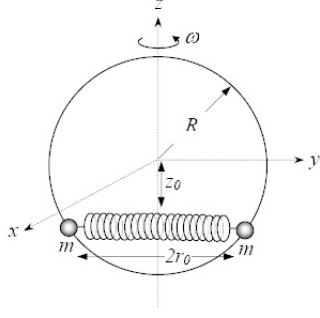


Figure 1: BHS model. Two beads attached by a spring slide without friction along a horizontal hoop with rotation. The beads have the same position  $z_0$  from the center.

center of the hoop. There are two equivalent equilibrium positions determined by the transformation  $z_0 \rightarrow -z_0$ , which illustrates the presence of a discrete symmetry. The hoop rotates about the  $z$  axis at angular velocity  $\omega$ , which causes the equilibrium position  $z_0$  to decrease and the spring to stretch from its natural length  $2r_0$  to a longer length  $2r$ . The lagrangian contains the kinetic energy of each bead and the elastic potential of the spring, while the gravitational potential is not considered because the center of mass of the system lies along the horizontal axis  $z$ . It is more suitable to write the lagrangian in cylindrical coordinates, which displays in a simpler form the symmetries and constraints of the system. The lagrangian is then written as

$$L = m(\dot{r}^2 + r^2\dot{\phi}^2 + \dot{z}^2) - 2k(r - r_0)^2. \quad (1)$$

The change in time of the azimuthal angle  $\phi$  is identified as the angular velocity of the hoop. We can eliminate the coordinate  $r$  through the constraint  $r = \pm\sqrt{R^2 - z^2}$  which indicates that the motion of the beads is restricted along the hoop. Hence, the lagrangian can be expressed in terms of the generalized coordinate  $z$  as

$$L = \frac{1}{2}\mu\dot{z}^2 - V_{ef}(z), \quad (2)$$

where we have defined an effective mass  $\mu = \frac{2mR^2}{R^2 - z^2}$  and a one-dimensional effective potential given by

$$V_{ef}(z) = V_{el} - V_{cent} = 2k(\sqrt{R^2 - z^2} - r_0)^2 - m\omega^2(R^2 - z^2), \quad (3)$$

with  $V_{el}$  the elastic potential of the spring and  $V_{cent}$  the centrifugal potential which contains the rotational dynamics. It is evident that the lagrangian in (2) does not change under the coordinate transformation  $z \rightarrow -z$ . The introduction of the effective potential in Eq. (3) will help

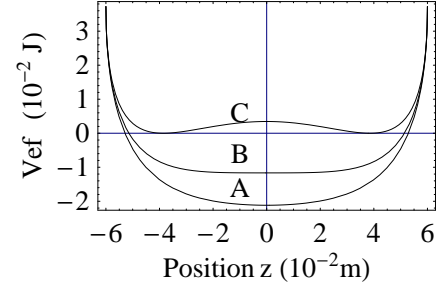


Figure 2: Effective potential as a function of the  $z$  coordinate for angular velocity (A)  $\omega > \omega_c$ , (B)  $\omega = \omega_c$  and (C)  $\omega < \omega_c$ .

us to determine the stability behavior of the system. Equilibrium occurs when

$$\frac{dV_{ef}}{dz} = 4kzr_0 \left( \frac{1}{\sqrt{R^2 - z^2}} - \frac{1}{\xi} \right) = 0, \quad (4)$$

where  $\xi(\omega) = \frac{2kr_0}{2k - m\omega^2}$ . The condition (4) determines 3 equilibrium points at

$$z_0 = 0 \quad \text{and} \quad \pm\sqrt{R^2 - \xi^2}. \quad (5)$$

To investigate the stability of the solutions above, we must examine the second derivative of the effective potential, which gives

$$\frac{d^2V_{ef}}{dz^2} = 4kr_0 \left[ \frac{R^2}{(R^2 - z^2)^{3/2}} - \frac{1}{\xi} \right]. \quad (6)$$

This expression evaluated in the 3 equilibrium points, displays different possibilities according to the sign of the second derivative. The results are resumed in table I, where  $R^2 \geq \xi^2$  was demanded in order to assure real solutions for  $z_0 = \pm\sqrt{R^2 - \xi^2}$ . In Fig. 2 we show three different plots of the effective potential as a function of the coordinate  $z$ , where we distinguish a critical angular velocity determined by

$$\omega_c^2 = \frac{2k(R - r_0)}{mR}, \quad (7)$$

and two regions that depend on the value of the angular velocity of the hoop. For values with  $\omega^2 > \omega_c^2$  (symmetrical phase), there is just one minimum at  $z = 0$  that corresponds to the case in which both beads hold their maxima distance in a symmetrical position. When the angular velocity slowly decreases near to the value determined by  $\omega^2 = \omega_c^2$ , the minimum of energy becomes flatter. Immediately below the critical value  $\omega_c$ , the single minimum bifurcates into two degenerated minima  $z = \pm\sqrt{R^2 - \xi^2}$  with the same energy. However, the spring chooses one of the minima causing an spontaneously symmetry breaking,

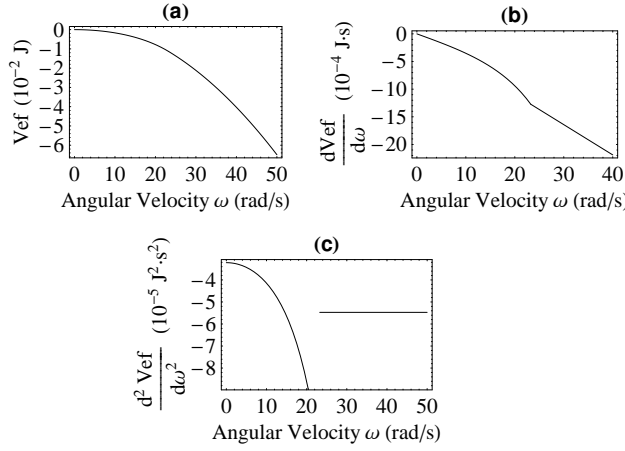


Figure 3: Analytical behavior of the effective potential with the angular velocity. (a) and (b) show the continuity of  $V_{ef}$  and  $\frac{dV_{ef}}{d\omega}$ . (c) displays an infinite discontinuity across the critical point  $\omega_c$  (in these plots is  $23.26 \text{ rad/s}$ ), exhibiting a second-order phase transition.

where the symmetry transformation  $z \rightarrow -z$  is not manifest, and the spring comes to a new equilibrium position in either a positive or a negative coordinate  $z$ , which is greater with decreasing  $\omega$ . Thus, the absolute value of  $z$  measures the degree of breaking just like an order parameter.

We can describe this process like a second order phase transition if we investigate the behavior of the effective potential in the critical point with respect to the variation of the angular velocity. The Ehrenfest definition establish that a phase transition with respect to a thermodynamic variable (like temperature) is of  $n^{\text{th}}$  order if the energy and its  $(n-1)$ st-order derivatives are continuous at the transition point, whereas the  $n^{\text{th}}$ -order derivative suffers a finite discontinuous jump. In fact, our system presents continuous derivative at first-order but suffers an infinite discontinuity in the second-order derivative  $\frac{d^2V_{ef}}{d\omega^2}$  as is shown in Fig. 3, where the angular velocity  $\omega$  works like the temperature in a thermodynamic system. The infinite jumps are described by the Tisza's Theory [3] which describes most of the higher-order phase transition.

We emphasize that this behavior is analogous but not

Angular Vel.	Equilib. points	Stability
$\omega^2 > \frac{2k(R-r_0)}{mR}$	$z_0 = 0$	$\frac{d^2V_{ef}}{dz^2} > 0$ stab.
$\omega^2 = \frac{2k(R-r_0)}{mR}$	$z_0 = 0$	$\frac{d^2V_{ef}}{dz^2} = 0$ undef.
$\omega^2 < \frac{2k(R-r_0)}{mR}$	$z_0 = 0$ $z_0 = \pm\sqrt{R^2 - \xi^2}$	$\frac{d^2V_{ef}}{dz^2} < 0$ unstb. $\frac{d^2V_{ef}}{dz^2} > 0$ stab.

Table I: Stability regions according to the angular velocity. There is a critical angular velocity that separates two different phases.

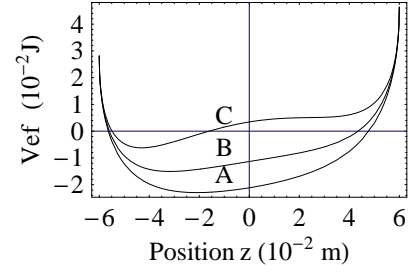


Figure 4: Effective potential as a function of the  $z$  coordinate for angular velocity (A)  $\omega > \omega_c$ , (B)  $\omega = \omega_c$  and (C)  $\omega < \omega_c$ . The gravity causes the negative minimum to be lower.

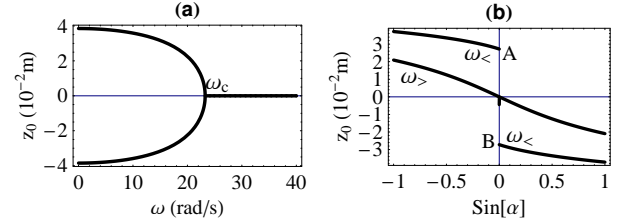


Figure 5: Projections of phase diagram in the (a)  $z_0 - \omega$  and (b)  $z_0 - \text{Sin}[\alpha]$  planes. The "iso-velocities" in (b) show a first-order transition for  $\omega < \omega_c$ , where  $z_0$  jumps discontinuously between A and B.

equal to the SSB in quantum theory. The analogy arises when the minimum of energy splits into new degenerated minima. Nonetheless, classically the system will maintain its symmetrical unstable equilibrium unless there appears external fluctuations that are not being considered into the equation of motion (in this sense this is not a "true" SSB). On the other hand, the quantum theory introduces fluctuations associated with the uncertainty principle inherent into the structure of the theory. Such fluctuations appear spontaneously to unbalance the system toward a not symmetrical state.

If the horizontal hoop is turned into an angle  $\alpha$ , the gravity induces an explicit symmetry breaking. In this case the effective potential in (3) changes as

$$V_{ef}(z) = 2k \left( \sqrt{R^2 - z^2} - r_0 \right)^2 - m\omega^2 (R^2 - z^2) + 2mgz \text{Sin}\alpha, \quad (8)$$

where the last term corresponds to the gravitational potential of both beads. The zero gravitational potential is taken in the symmetrical point  $z = 0$ . It is clear that Eq. (8) does not hold the symmetry  $z \rightarrow -z$  due to the gravitational term, which will favor negative positions with lower energy. In this case, the symmetrical plots from Fig. 2 will suffer slight deformations, such as is illustrated in Fig. 4, where we can see that for  $\omega < \omega_c$  the minima splits into two different values as local and global minima. This behavior is observed, for instance, in an atom or molecule that presents a degenerated spectrum of energy due to the spherical symmetry. If there

are external fields such as electric or magnetic fields, this spectrum splits into many distinguished levels of energies (Stark and Zeeman effect). We can obtain a phase diagram from the minima conditions. When the axis of rotation is in horizontal position, the minima solutions in Eq. (5) as a function of  $\omega$  describes a plot analogous to the

magnetization-temperature phase diagram in a ferromagnet, such as Fig. 5(a) shows. If the z-axis holds different angles  $\alpha$  with respect to the horizontal plane, the minimum condition from the effective potential in Eq. (8) describes a diagram as a function of  $\sin\alpha$  similar to the isotherms in a magnetization-magnetic field phase diagram (see Fig. 5(b)). When  $\omega < \omega_c$ , Fig. 5(b) illustrates how the global minimum jumps discontinuously from  $-z_0$  to  $z_0$  when  $\alpha$  passes through zero, like a first-order transition.

### III Critical Exponents

Above, we identified the equilibrium position  $z_0$  as the parameter of order which measures the degree of breaking of the symmetry. The behavior of second-order transition suggests us a critical behavior near the transition point. The effective potential from Eq. (3) can be written as

$$V_{ef}(z) = 2k(R^2 + r_0^2) - m\omega^2 R^2 + (m\omega^2 - 2k)z^2 - 4kr_0 R \sqrt{1 - \left(\frac{z}{R}\right)^2}. \quad (9)$$

Since nearly below the critical point  $\omega_c^2 = \frac{2k(R-r_0)}{mR}$  the minimum at  $z_0 = 0$  suffers small deviation  $z \approx \pm \delta z$ , we can expand the root term in (9) as  $\sqrt{1 - \left(\frac{z}{R}\right)^2} = 1 - \frac{1}{2}\left(\frac{z}{R}\right)^2 - \frac{1}{8}\left(\frac{z}{R}\right)^4 - \dots$ , so that the effective potential takes the form of a Landau-type expansion near the critical point

$$V_{ef}(z_0) = a_0 + a_2 z^2 + a_4 z^4 + \dots, \quad (10)$$

where the coefficients up to fourth order are

$$a_0 = -\left[\omega^2 - \left(\frac{R-r_0}{R}\right)\omega_c^2\right]mR^2 \quad (11a)$$

$$a_2 = m(\omega^2 - \omega_c^2) \quad (11b)$$

$$a_4 = \frac{kr_0}{2R^3}, \quad (11c)$$

Furthermore, near  $\omega_c$  the coefficient in (11b) becomes

$$a_2 \approx 2m\omega_c(\omega - \omega_c) = a_2^0(\omega - \omega_c). \quad (12)$$

The Landau theory [4] is formulated in the framework of the mean-field approximation, which in our case takes the form of a minimum condition. Thus, the potential in (10) up to fourth order must accomplish the condition

$$\frac{dV_{ef}(z_0)}{dz} = z_0 [2a_2^0(\omega - \omega_c) + 4a_4 z_0^2] = 0. \quad (13)$$

For  $\omega > \omega_c$  the only real solution is  $z_0 = 0$ , while for  $\omega < \omega_c$  two real minima solutions are obtained

$$z_0 = \pm \left[ \frac{a_2^0}{2a_4} (\omega_c - \omega) \right]^{1/2}. \quad (14)$$

Thus, the parameter of order spontaneously becomes nonzero and grows as  $\sqrt{\omega_c - \omega}$  for angular velocities nearly below  $\omega_c$ . The critical exponent  $\beta = \frac{1}{2}$  associated with the order parameter is identical to those obtained by the classical Landau theory for thermodynamic parameters [4, 5], such as the magnetic moment in a ferromagnetic substance, the difference in Zn-Cu occupation in a binary alloy, the molar volume liquid-gas in a fluid, among other second-order transitions.

This system could be thought as a mechanical equivalent of a thermodynamic system, where the state is characterized by three "thermodynamic" variables: the equilibrium position  $z_0$  (parameter of order), the angular velocity  $\omega$  (temperature-like variable) and the gravitational force (pressure-like variable). A change of state can take place if we introduce a "heat reservoir", which in our case is a power source (for example an electric motor) that provides the rotational energy to the hoop. If we consider the complete potential including the gravitational coupling  $W = 2mg\sin\alpha$ , the condition in Eq. (13) takes the form

$$\frac{dV_{ef}(z_0)}{dz} = 2a_2^0(\omega - \omega_c)z_0 + 4a_4 z_0^3 + W = 0. \quad (15)$$

	BHS-System	Ferromagnet (Ising model)
Broken Symmetry	Mirror reflection $z \rightarrow -z$	Spin reflection $s \rightarrow -s$
Critical Point	$\omega_c =  z_{0(\omega \rightarrow 0)}  \sqrt{\frac{2k}{mR(R+r_0)}}$	$T_c =  M_{(T \rightarrow 0)}  \frac{q\mu_0}{k_B}$
Parameter of Order (near critical point)	$z_0 = \begin{cases} 0, & (\omega > \omega_c) \\ \pm z_{0(\omega \rightarrow 0)} \sqrt{\frac{4R^2}{r_0(R+r_0)}} \left[ \frac{\omega_c - \omega}{\omega_c} \right]^{1/2}, & (\omega < \omega_c) \end{cases}$	$M = \begin{cases} 0, & (T > T_c) \\ \pm M_{(T \rightarrow 0)} \sqrt{3} \left[ \frac{T_c - T}{T_c} \right]^{1/2}, & (T < T_c) \end{cases}$
Conjugate Field	Gravitational Field: $2mg\sin\alpha$	Magnetic Field $H$
Susceptibility	$\chi_{mech} = \begin{cases} \frac{-R}{8k(R-r_0)} \left( \frac{\omega - \omega_c}{\omega_c} \right)^{-1}, & (\omega > \omega_c) \\ \frac{-R}{16k(R-r_0)} \left( \frac{\omega_c - \omega}{\omega_c} \right)^{-1}, & (\omega < \omega_c) \end{cases}$	$\chi_{magn} = \begin{cases} \frac{1}{q} \left( \frac{T - T_c}{T_c} \right)^{-1}, & (T > T_c) \\ \frac{1}{2q} \left( \frac{T_c - T}{T_c} \right)^{-1}, & (T < T_c) \end{cases}$

Table II: Comparison between mechanical and ferromagnetic systems.  $M$  is the magnetic moment,  $k_B$  the Boltzmann's constant,  $\mu_0$  the Bohr magneton and  $q$  the coupling constant of a mean field (which is the magnetic equivalent to the spring constant  $k$ ).

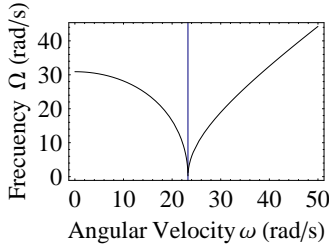


Figure 6: Frequency of oscillation as function of  $\omega$ . At  $\omega_c$ , the frequency becomes zero. Above  $\omega_c$  the frequency  $\Omega_>$  grows with  $\omega$  without limit, while below, the frequency  $\Omega_<$  grows as  $\omega$  decreases

The mechanical susceptibility, which is understood as the linear response of the parameter of order (minimum position  $z_0$ ) due to an infinitesimal conjugate field ( $W$ ) is  $\chi_{mech} = \frac{\partial z_0}{\partial W}$ . This can be calculated if we differentiate the Eq. (15) with respect to  $W$ , obtaining

$$\chi_{mech} = \frac{-1}{2a_2^0(\omega - \omega_c) + 12a_4z_0^2} = \begin{cases} \frac{-1}{2a_2^0}(\omega - \omega_c)^{-1}, & \text{for } \omega > \omega_c \\ \frac{-1}{4a_2^0}(\omega_c - \omega)^{-1}, & \text{for } \omega < \omega_c \end{cases} \quad (16)$$

from which we deduce the critical exponent  $\gamma = 1$ . Table II lists several corresponding features between the mechanical and the ferromagnetic system in the framework of the two-dimensional Ising model under the Mean-Field approximation [6]. The results are listed in terms of the equilibrium positions at  $\omega = 0$  ( $z_0(\omega \rightarrow 0)$ ) and the magnetization at  $T = 0$  ( $M(T \rightarrow 0)$ ).

## IV Small Oscillations

We can study small oscillations about the equilibrium positions. For the symmetrical phase with  $\omega > \omega_c$ , the effective potential in (3) can be expanded in a Taylor's series about the minimum at  $z = 0$ , from where we obtain an harmonic potential given by

$$V_{ef}(\delta z) \approx \text{cons.} + 2kr_0 \left( \frac{1}{R} - \frac{1}{\xi} \right) (\delta z)^2 = \text{cons.} + \frac{k_{ef}}{2} (\delta z)^2, \quad (17)$$

where we can identify an effective spring constant  $k_{ef} = 4kr_0 \left( \frac{1}{R} - \frac{1}{\xi} \right)$ . We can even identify the effective mass defined by the Eq. (2) at  $z = 0$  as  $\mu = 2m$ . Then, the frequency of oscillation above the critical point is  $\Omega_> = \sqrt{\frac{k_{ef}}{\mu}} = \sqrt{\frac{2kr_0}{m} \left( \frac{1}{R} - \frac{1}{\xi} \right)}$ , where  $|\xi| > |R|$ . The frequency  $\Omega_>$  approaches zero near  $\omega_c$ , and the period of oscillation becomes infinite in the threshold of stability at  $z = 0$  (see Fig. 6). This frequency increases without limit with  $\omega$ . For the breaking phase with  $\omega < \omega_c$ , we can perform a similar analysis about the minima at  $z = \pm \sqrt{R^2 - \xi^2}$ . In this case, the effective constant is  $k_{ef} = 4kr_0 \left( \frac{R^2}{\xi^3} - \frac{1}{\xi} \right)$

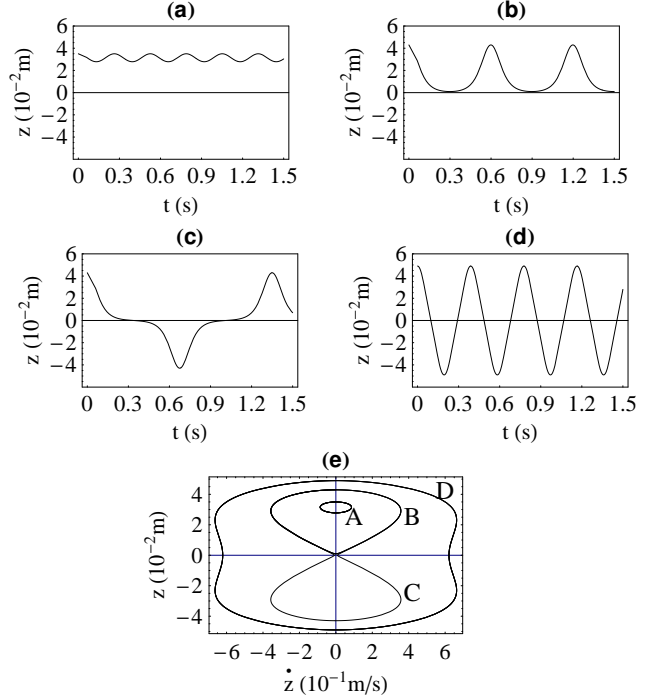


Figure 7: Graphical solutions for  $\omega < \omega_c$ . The position as a function of time is shown for (a) small perturbations at  $z > 0$ , greater perturbations just (b) below and (c) above the jump over  $z = 0$ , and (d) for enormous perturbations. Each solution (A,B,C and D respectively) is shown (e) in the phase space.

and the effective mass is  $\mu = 2m \frac{R^2}{\xi^2}$ . Hence, the frequency is  $\Omega_< = \sqrt{\frac{2kr_0}{m} \left( \frac{1}{\xi} - \frac{\xi}{R^2} \right)}$  where  $|\xi| < |R|$ . Here, as  $\omega$  decreases, the function  $\xi(\omega)$  decreases and reaches its minimum value at  $\xi = r_0$  when the hoop comes to a complete rest with  $\omega = 0$ . As the angular velocity decreases, the frequency  $\Omega_<$  below the critical value becomes greater and reaches its maximum value  $\Omega_< = \sqrt{\frac{2k}{m} \left( 1 - \left( \frac{r_0}{R} \right)^2 \right)}$  when  $\omega = 0$ .

## V Chaotic Behavior

The complete description of the system is obtained as solution from the Lagrange's equations associated with the generalized coordinate  $z$

$$\frac{d}{dt} \left( \frac{\partial L}{\partial \dot{z}} \right) - \frac{\partial L}{\partial z} = 0. \quad (18)$$

With the lagrangian defined by Eq. (2) and the effective potential from Eq. (3), we obtain the equation of motion

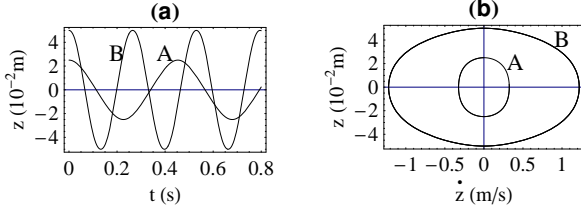


Figure 8: Graphical solutions for  $\omega > \omega_c$ . The position as a function of time is shown in (a) for (A) small perturbations and (B) greater perturbations. Each solution (A and B respectively) is shown (b) in the phase space.

$$\ddot{z} + \left( \frac{z}{R^2 - z^2} \right) \dot{z}^2 + \left( \frac{2k}{mR^2} - \frac{\omega^2}{R^2} \right) z^3 + \frac{2kr_0}{mR^2} z \sqrt{R^2 - z^2} - \left( \frac{2k}{m} - \omega^2 \right) z = 0, \quad (19)$$

which is a quite complex equation to solve. We note that this equation involves non-linear terms, which suggests us a chaotic behavior. From data given in Sec. VI, we consider numerical solutions with different initial positions around the equilibrium points (the entrance  $\dot{z}(0)$  was always taken zero). Figs. in 7 display the behavior of the position  $z$  as function of time and in the phase space ( $z$  Vs.  $\dot{z}$ ) for  $\omega < \omega_c$ . We see clearly that for small perturbations, the oscillations are restricted in regions with  $z > 0$ . In the phase space, this motion describes elliptic-like paths (we also see that these paths are not perfect ellipses due to anharmonic terms). If we increase the perturbation, the system reaches the transition point, where the spring just oversteps the local maximum at  $z = 0$ , and the oscillations extend to both regions. For greater perturbations, the motion increases around all the hoop.

On the other hand, we can see in Fig. 8 that for  $\omega > \omega_c$ , the motion is developed around the equilibrium point at  $z = 0$ , in agreement with the results of Sec. IV. Figs. in 9 represent solutions for a value below but near the critical value, where we introduced small perturbations. For a slight perturbation ( $\delta z_0 \sim 5.92 \times 10^{-3} m$ ), the system develops a motion in the breaking region. But if this perturbation is changed into  $\delta z_0 \sim 6.926 \times 10^{-3} m$ , the system presents random oscillations between both regions, where the graphs in the phase space describes chaotic paths. The pattern of this chaotic behavior is in extrem sensitive to very tiny changes of initial conditions (with differences of just  $\sim 1 \times 10^{-13} m$ ). Exactly on the critical value (Fig. 10), the system presents very long and irregular oscillations.

## VI Experimental Description

We made a demonstrative BHS-apparatus using a hoop with radius  $R = 6$  cm, a soft spring with natural length

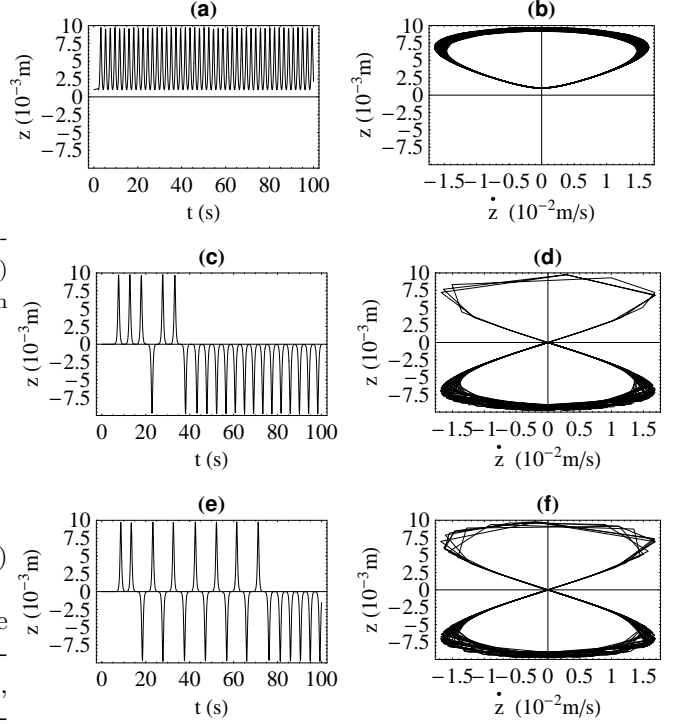


Figure 9: Graphical solutions for  $\omega$  slightly below  $\omega_c$ . The position as a function of time is shown for (a) very small perturbations at  $z > 0$  and (c), (e) greater perturbations. Each solution ((b), (d) and (f) respectively) is shown in the phase space. These plots exhibit a chaotic behavior.

$r_0 = 4.6$  cm and constant  $k = 8.81$  N/m, and two iron rings used as beads, each one with mass  $m = 7.6$  g. The hoop was coupled to the axis of a DC motor with adjustable velocity (which will work like a "heat reservoir").

Aligning the rotational axis in a horizontal position, the system describes the two regimes of symmetry. The experimental observation is illustrated in Fig. 11 according to the angular velocity. The measured critical velocity was  $\omega_c = 25.24 \pm 2.1$  rad/s ( $241 \pm 20$  RPM), which is in a quite good agreement with the results from table I, where a critical point at  $\omega_c = 23.26$  rad/s ( $222.1$  RPM) is expected. In addition to the motion at  $\omega_c$ , Fig. 11 shows two cases with  $\omega < \omega_c$  and one case with  $\omega > \omega_c$ . When the velocity was decreased below the critical value, we noted that the chosen direction ( $+z$  or  $-z$ ) was highly sensitive to the way that the velocity was reduced and to the mechanical fluctuations near the transition. When the velocity was slowly reduced in a quasi-static process across the transition, the equilibrium position was maintained at  $z = 0$  (although we lubricate the hoop, the unstable equilibrium found some stability due to the small friction), but after some hesitating seconds the system finally fell into one of the stable minima (long relaxation time), breaking the symmetry. However after several trials, we could see that the symmetry was hidden in the sense that we obtained about the same number of breakings into  $+z$  as



into  $-z$ , i.e. both possibilities have the same probability of occurrence. Thus, we can see how the symmetry breaking is spontaneous, where the non-symmetrical states present two equally probable possibilities with the same energy. On the other hand, the device had a high sensitivity to the precision of the horizontal alignment. When the rotational axis was slightly deviated with  $\omega > \omega_c$ , the system always shows a breaking in one direction due to the gravitational potential, in agreement with the behavior described by Fig. 4. We estimated experimental explicit breaking within a range  $\alpha < 0.1 \text{ rad}$  ( $\lesssim \pm 5^\circ$ ).

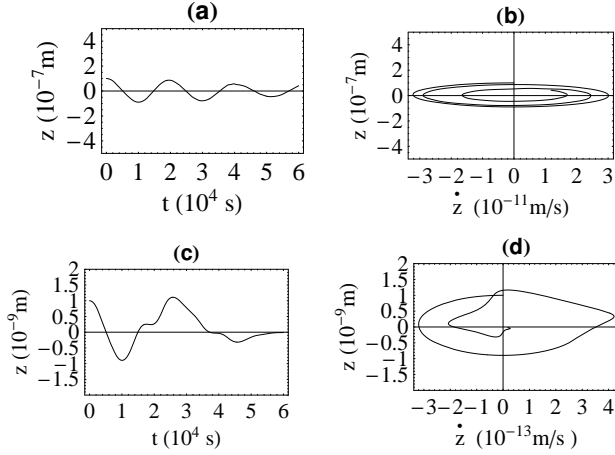


Figure 10: Graphical solutions for  $\omega = \omega_c$ . The position as a function of time is shown for (a),(c) small perturbations. Each solution ((b) and (d) respectively) is shown in the phase space. These plots exhibit a long oscillation with chaotic behavior.

## VII Summary and Conclusions

In this work we studied a bead-hoop-spring (BHS) system under rotation as was described through the sections. The system presents different stability situations according to the angular velocity of the hoop, exhibiting a second order transition behavior, and where the position  $z_0$  of the center of mass measured from the center of the hoop defines a parameter of order. The symmetry transformation  $z \rightarrow -z$  of the lagrangian is manifest if the angular velocity is above a critical value  $\omega_c$ , where the equilibrium position at  $z_0 = 0$  is stable. Below  $\omega_c$ , this equilibrium becomes unstable, and appears two degenerated minima with  $z_0 \neq 0$ . Thus, with only internal interactions (spring force and normal force between hoop and beads), the system exhibits an SSB below the critical value. If the gravitational potential is considered, the stability regions suffer a deformation, changing the equilibrium position at  $z = 0$  into another different from zero, and splitting the minima of energy at  $z_0 \neq 0$  into two non-equivalent minima. Under these circumstances, the system shows a preferential direction exhibiting explicit symmetry breaking and a first-

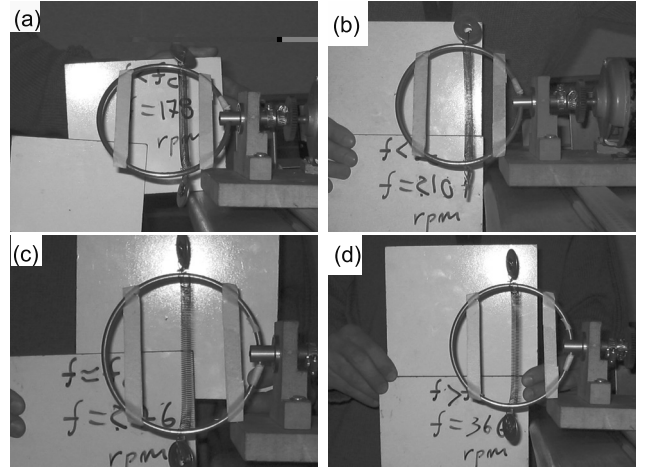


Figure 11: Experimental device for frequency of rotation (a)  $f = 178 \text{ RPM}$  ( $\omega = 18.64 \text{ rad/s}$ ), (b)  $f = 210 \text{ RPM}$  ( $\omega = 21.99 \text{ rad/s}$ ), (c)  $f = 246 \text{ RPM}$  ( $\omega = 25.13 \text{ rad/s} \approx \omega_c$ ) and (d)  $f = 366 \text{ RPM}$  ( $\omega = 38.32 \text{ rad/s} > \omega_c$ ).

order transition behavior. The experimental observations were in quite good agreement with the theoretical description, where the critical velocity was measured within an 8% of precision.

The system belongs to the same universality class that many thermodynamic systems, exhibiting a Landau expansion. From a mean-field-like approximation, we obtained the critical exponent  $\beta = \frac{1}{2}$  and  $\gamma = 1$  associated with the parameter of order and the "mechanical susceptibility" respectively.

The frequency of small oscillations about the stable minima was also calculated. Above  $\omega_c$ , the frequency  $\Omega_>$  increases without limit with  $\omega$ . Near the critical value, the motion about  $z = 0$  describes long-period oscillations, which becomes into unbounded motion when  $\omega$  passes through the critical point. Below  $\omega_c$ , the frequency  $\Omega_<$  about the new minima increases with  $\omega$  decreases.

The equation of motion exhibits some chaotic behavior near the critical value, where the system reacts in a random way for similar perturbation entrance.

This analogy between the mechanical system and a thermodynamic system is highly suggestive, and it is very tempter to apply a deeper study of fluctuations below the critical point through the definition of a correlation function and the implementation of a fluctuation-dissipation theorem [4, 5], which could provide some insights about the physical sense of these concepts.

## Acknowledgment

We thank Rodolfo Diaz and William Herrera from Universidad Nacional de Colombia for their comments, which improve the content of this paper. We also thank to Mr. Francisco and Yuri from Escuela Colombiana de Ingeniería for their collaboration in the development of the experi-

mental device.

- [1] For a brief introduction to gauge theory in classical and quantum mechanics see C. Cohen-Tannoudji, B. Diu, F. Laloe *Quantum Mechanics* (Wiley-Interscience Publication, 1986), pp. 315-328. In particle physics see W. Greiner and B. Müller, "Gauge Theories of Weak Interactions," (Springer, 1996).
- [2] T. Bernstein, Am. J. Phys. **39**, 832-839 (1971); R. Alben, Am. J. Phys. **40**, 3-8 (1972); E. Guyon, Am. J. Phys. **43**, 877-881 (1975); J. Sivardiere, Am. J. Phys. **51**, 1016-1018 (1983); V.H. Schmidt and B.R. Childelrs, Am. J. Phys. **52**, 39-43 (1984); J.R. Drugowich de Felicio and O. Hipolito, Am. J. Phys. **53**, 690-693 (1985); J.E. Drumheller, D. Raffaele and M. Baldwin, Am. J. Phys. **54**, 1130-1133 (1986); G. Fletcher, Am. J. Phys. **65**, 74-81 (1996); J. Mahecha and L.A. Sánchez, Rev. Mex. Fís. **49** (4), 364-370 (2003).
- [3] H.B. Callen, *Thermodynamics* (John Wiley & Sons, 1960).
- [4] L.D. Landau and E.M. Lifshitz, *Statistical Physics* (Pergamon Press, 1980) Vol. 5, Part 1, 3<sup>rd</sup> ed.
- [5] K. Huang, *Statistical Mechanics* (John Wiley & Sons, 1987), 2<sup>nd</sup> ed.
- [6] The magnetic model (Curie-Weiss model) is proposed as an instructive exercise in ref. [5], Problem 14.3, pp. 364.